RSC Advances

ROYAL SOCIETY OF CHEMISTRY

www.rsc.org/advances

Synthesis and characterization of polystyrene-*graft*-polythiophene via a combination of atom transfer radical polymerization and Grignard reaction

Maryam Hatamzadeh[1], and Mehdi Jaymand[*, 2]

1. Department of Chemistry, Payame Noor University, P.O. Box 19395-3697, Tehran, I.R., Iran.
2. Research Center for Pharmaceutical Nanotechnology, Tabriz University of Medical Sciences, P.O. Box 51656-65811, Tabriz, I.R., Iran.

[*] Correspondence to: Mehdi Jaymand, Research Center for Pharmaceutical Nanotechnology, Tabriz University of Medical Sciences, Tabriz, Iran

Tel: +98-411-3367914; Fax: +98-411-3367929

Postal address: Tabriz-5165665811-Iran

E-mail addresses: m_jaymand@yahoo.com; m.jaymand@gmail.com; jaymandm@tbzmed.ac.ir

Abstract

In this paper, a new strategy for synthesis of polystyrene-*graft*-polythiophene (PSt-*g*-PTh) is explored. For this purpose, first poly(styrene-*co*-acrylonitrile) (PSt-*co*-PAN) was synthesized via atom transfer radical polymerization (ATRP), and then the nitrile groups of acrylonitrile units were converted to thiophene groups using Grignard reaction between 2-thienylmagnesium bromide and nitrile groups to produce a thiophene-functionalized polystyrene macromonomer (ThPStM). The graft copolymerization of thiophene monomers onto polystyrene backbone was initiated by oxidized thiophene groups after addition of ferric chloride ($FeCl_3$), an oxidative catalyst for polythiophene synthesis, and $FeCl_3$-doped polythiophene was chemically grafted onto polystyrene backbone via oxidation polymerization. The graft copolymer obtained was characterized by ^1H nuclear magnetic resonance (NMR), and Fourier transform infrared (FTIR) spectroscopy, and its electroactivity behavior was verified under cyclic voltammetric conditions. Moreover, thermal behaviors of the synthesized polymers were investigated by means of differential scanning calorimetry (DSC), and thermogravimetric analysis (TGA).

Keywords: Polystyrene, Atom transfer radical polymerization, Grignard reaction, Polythiophene, Graft copolymer, Modification

1. Introduction

It is a decisive fact that intrinsically conductive polymers (ICPs) have stimulated great interest on the basis of their importance in basic scientific research and potential industrial applications, due to their unique semiconducting and optoelectronic properties [1-7]. In particular, conjugated polythiophene (PTh) stands out as one of the most promising members of the conjugated polymer family because of its significant and remarkable properties such as low-cost synthesis, excellent environmental and thermal stability, mechanical strength, magnetic and optical properties, as well as its wide range of applications [8-13]. The conjugated polythiophene and its derivatives have potential applications in sensors [14, 15], organic photovoltaics (OPVs) [16, 17], organic field-effect transistors (OFETs) [18, 19], organic light emitting diodes (OLEDs) [20, 21], and biomedical fields [22, 23]. Polythiophene and its derivatives can be synthesized via electrochemical polymerization [24, 25], condensation polymerization with or without organometallic reagents [26, 27], and chemical oxidation polymerization [28, 29], of corresponding monomers.

However, the main drawback of unsubstituted polythiophene is the lack of solubility, which explains its limited processablity due to its rigid backbone. In order to overcome these major deficiencies, well-established techniques are: (i) side chain functionalization [30, 31], usually at the β-carbons, (ii) synthesis of polythiophene copolymers with conventional thermoplastics [32, 33], and (iii) combination of both aforementioned approaches [34, 35]. Currently, to the best of our knowledge, most of the reported approaches prepare unsubstituted polythiophene copolymers via free radical polymerization of monomers with thiophene moiety and then oxidative polymerization

with $FeCl_3$ from the backbone. It is difficult to control the dispersity index (Đ $= \overline{M}_w / \overline{M}_n$), and the structure of the copolymers. These copolymers show poor fluorescent ability probably due to the severe stacking of polythiophene chains [36-39].

These problems can be circumvented through atom transfer radical polymerization (ATRP), as well as other reversible-deactivation radical polymerization (RDRP) techniques. Atom transfer radical polymerization technique has been one of the most efficient reversible-deactivation radical polymerization methods since its introduction by Wang and Matyjaszewski [40]. The controlled chain growth and 'living' nature of ATRP make it very powerful tool for the synthesis of well-defined graft and block copolymers. Another advantage of this approach over conventional free radical polymerizations is that only negligible homopolymer can be observed when employed in graft copolymerization [41]. ATRP has many advantages over other RDRP techniques such as easy experimental setup, its applicability to monomers possessing various functional groups and polarities, and its tolerance to many solvents, additives, and impurities often encountered in industrial systems [42-44]. Among reversible-deactivation radical polymerization techniques, ATRP is the most commonly used approach toward synthesis of PTh copolymers with conventional thermoplastics [45-48].

For the first time, synthesis and characterization of polystyrene-*graft*-polythiophene (PSt-*g*-PTh) via a combination of atom transfer radical polymerization (ATRP), and Grignard reaction is reported. For this purpose, first poly(styrene-*co*-acrylonitrile) (PSt-*co*-PAN) was synthesized via ATRP, and then the nitrile groups of acrylonitrile units were converted to thiophene groups using Grignard reaction between 2-thienylmagnesium

bromide and nitrile groups. The synthesized macromonomer (ThPStM) was subsequently used in the graft copolymerization of thiophene monomers onto polystyrene backbone via chemical oxidative polymerization in the presence of anhydrous $FeCl_3$ to produce a PSt-*g*-PTh graft copolymer.

2. Experimental

2.1. Materials

Styrene, acrylonitrile, and thiophene monomers from Merck (Darmstadt, Germany) were distilled under reduced pressure before use. Benzene, toluene, and tetrahydrofuran (THF) (Merck) were dried by refluxing over sodium and distilled under argon prior to use. Ferric chloride, 2,2′-bipyridyl (Bpy), 2-bromothiophene, tetraethylammonium tetrafluoroborate (TBAFB), and methyl 2-bromopropionate (Merck), were used as received. Cuprous bromide (CuBr) was purified by stirring in glacial acetic acid, washing with methanol, and then drying under vacuum at 50 °C. All other reagents were purchased from Merck and purified according to standard methods.

2.2 Synthesis of poly(styrene-*co*-acrylonitrile) via ATRP technique

In a dry ampoule were charged with toluene (20 mL), styrene (10.35 mL, 90 mmol), acrylonitrile (0.65 mL, 10 mmol), CuBr (0.14 g, 1 mmol), 2,2′-bipyridyl (Bpy) (0.31 g, 2 mmol), and methyl 2-bromopropionate (0.033 mL, 0.3 mmol). The ampoule was degassed with several freeze–pump–thaw cycles and sealed off under vacuum and placed in an oil bath at 90 °C. During the reaction, the viscosity of the mixture was observed to gradually increase. After 12 hours, the product was cooled, diluted with tetrahydrofuran (THF), and the obtained solution was passed through a column filled with neutral alumina in order to remove the copper catalyst. The polymer was precipitated in excess

methanol. The product was dried overnight under vacuum at room temperature (Scheme 1). The acrylonitrile content in the copolymer was 3.9% (by mole) based on peak at 3.75 ppm (-CHCN) in the ^{1}H NMR spectrum.

(Scheme 1)

2.3. Synthesis of thiophene-functionalized polystyrene macromonomer (ThPStM)

A 100 mL flame-dried three-necked round-bottom flask (flask 1) containing 0.12 g (5 mmol) magnesium, 0.025 g (0.1 mmol) iodine, 0.33 mL (3.5 mmol) 2-bromothiophene, and dried THF (20 mL) was equipped with condenser, septum, gas inlet/outlet, and a magnetic stirrer, under an argon atmosphere. The mixture was refluxed at 60 °C under an argon atmosphere for about 24 hours.

At the end of this period, a separate 100 mL flame-dried three-necked round-bottom flask (flask 2) containing 2 g (19.5 mmol) of PSt-*co*-PAN in 20 mL of dried benzene was equipped with a condenser, septum, gas inlet/outlet, and a magnetic stirrer, under an argon atmosphere. The solution was de-aerated by bubbling highly pure argon for 20 minutes, and then the Grignard reagent (2-thienylmagnesium bromide, flask 1) was introduced with a syringe through the septum. The mixture was refluxed at 75 °C under an argon atmosphere for about 24 hours. The thiophene-functionalized polystyrene macromonomer (ThPStM) was separated by precipitation in excess methanol, filtered, washed several times with methanol and dried in vacuum at room temperature (Scheme 2).

(Scheme 2)

2.4. Graft copolymerization of thiophene onto thiophene-functionalized polystyrene

In a three-necked round-bottom flask equipped with condenser, dropping funnel, gas inlet/outlet, and a magnetic stirrer, 1 g (9.7 mmol) of macromonomer (ThPStM), and thiophene monomer (1.5 mL, 19.1 mmol) were dissolved in 60 mL of dried carbon tetrachloride (CCl_4). The solution was de-aerated by bubbling highly pure argon for 20 minutes. In a separate container 12.4 g (76.4 mmol) of ferric chloride ($FeCl_3$) was dissolved in 20 mL of dried acetonitrile (CH_3CN). The solution was de-aerated by bubbling highly pure argon for 20 minutes and was slowly added to the mixture under an argon atmosphere. The mixture was refluxed for 24 hours at room temperature under inert atmosphere. The reaction was terminated by pouring the contents of the flask into a large amount of methanol. The crude product was filtered and washed several times with methanol (Scheme 3).

The crude product was extracted with THF in a Soxhlet apparatus for 24 hours in order to remove pure polythiophene (PTh is slightly soluble in THF). The polymer solution was filtered and precipitated into excess methanol. Afterwards, the product was added into cyclohexane and refluxed at 40 °C to remove any residual ungrafted polystyrene chains. The synthesized PSt-*g*-PTh is partially soluble in cyclohexane, while ungrafted polystyrene is completely soluble in cyclohexane at 40 °C. The dark red solid was dried in vacuum at room temperature.

(Scheme 3)

2.5. Synthesis of polythiophene

The pure PTh was synthesized by a chemical oxidation polymerization method. The general procedure was as follows. In a three-necked round-bottom flask equipped with

condenser, dropping funnel, gas inlet/outlet, and a magnetic stirrer, 1.5 mL (19.1 mmol) of thiophene monomer was dissolved in 60 mL of dried CCl_4. The solution was de-aerated by bubbling highly pure argon for 20 minutes. In a separate container 12.4 g (76.4 mmol) ferric chloride was dissolved in 20 mL of dried CH_3CN. This solution was de-aerated by bubbling argon for 20 minutes and was slowly added to the mixture under an argon atmosphere. The mixture was refluxed for 24 hours at room temperature. At the end of this period, the precipitate was filtered off and washed several times with excess CH_3CN followed by acetone. The final black $FeCl_3$-doped polythiophene powder was obtained after drying at room temperature for 24 hours under reduced pressure (Scheme 4).

(Scheme 4)

2.6. Electrochemical system

The electrochemical studies were carried out using Auto-Lab equipment (ECO Chemie, Utrecht, The Netherlands) equipped with a three-electrode cell assembly. A platinum microelectrode (with a surface area of 0.03 cm^2), a platinum rod, and Ag/AgCl (1 M in KCl) were used as working, counter, and reference electrodes, respectively. The surface of the working electrode was polished with emery paper followed by 0.5 μm alumina, and then washed with acetone. To prepare the working electrode coated with the synthesized sample, the polymer was dissolved in THF to form a 1.0 mg mL^{-1} solution and ultrasonically treated for 10 minutes. The solution was dropped onto the platinum electrode surface and allowed to dry under ambient conditions. The electrochemical measurements were accomplished in the acetonitrile–tetraethylammonium tetrafluoroborate (TBAFB), solvent-electrolyte couple (0.1 mol L^{-1}) by applying a

sequential linear potential scan rate of 25–175 mVs^{-1} between 0.00 and +1.50 V *versus* the Ag/AgCl electrode. All experimental solutions were de-aerated by bubbling highly pure argon for 10 minutes, and an argon atmosphere was kept over the solutions during the measurements.

2.7. Characterization

The molecular weights of the obtained polymers (PSt-*co*-PAN and PSt-*g*-PTh) were determined by gel permeation chromatography (GPC) analysis with a Maxima 820 GPC Analysis Report (Ventura, CA, USA), using a polystyrene (10^6, 10^5 and 10^4 Å) calibration standard. Tetrahydrofuran (THF) was used as an eluent at a flow rate of 1 mL min^{-1} and column temperature of 25 °C. Fourier transform infrared (FTIR) spectra of the samples were obtained on a Shimadzu 8101M FTIR spectrometer (Shimadzu, Kyoto, Japan). The samples were prepared by grinding the dry powders with KBr and compressing the mixture into disks. The disks were stored in a desiccator to avoid moisture absorption. The spectra were recorded at room temperature. ^1H nuclear magnetic resonance (NMR) spectra were measured at room temperature using an FT-NMR (400 MHz) Bruker spectrometer (Bruker, Ettlingen, Germany). The sample for NMR spectroscopy was prepared by dissolving about 10 mg of the product in 1 mL of deuterated chloroform. The thermal properties of the samples were obtained with TGA-PL STA 1640 equipment (Polymer Laboratories, Church Stretton, Shropshire, UK). About 20 mg of the sample was heated between 25 and 800 °C at a rate of 10 °C min^{-1} under flowing nitrogen. Differential scanning calorimetry (DSC) analyses were performed on a Netzsch (Selb, Germany) DSC 200 F3 Maia. The sample was first heated to 200 °C and then allowed to cool for 5 minutes to eliminate the thermal history.

Thereafter, the sample was reheated to 200 °C at a rate of 10 °C min^{-1}. The entire test was performed under nitrogen purging at a flow rate of 50 mL min^{-1}. Ultraviolet–visible (UV–vis) spectroscopy was conducted using a Shimadzu 1601PC UV-vis spectrophotometer (Shimadzu, Kyoto, Japan) in the wavelength range 300–1000 nm. Electrochemical experiments were conducted using Auto–Lab PGSTA T302N. The electrochemical cell contained five openings: three of them were used for the electrodes and two for argon bubbling in the solutions during all experiments. The four-probe technique (Azar Electric, Urmia, Iran) was used to measure the conductivity of PTh and PSt-*g*-PTh samples at room temperature.

3. Results and Discussion

Creative design and developmental strategies of new polythiophenes has led to interesting new materials with improved physicochemical properties and potential for various technological applications. Among the various procedures for modification of unsubstituted polythiophene, synthesis of its copolymers with conventional thermoplastics is an efficient and versatile approach to prepare modified polythiophenes with specific properties through the proper selection of monomers and architectural design of the copolymer constituent monomers. It has been a scientific challenge and an industrially interesting subject to prepare graft or block copolymers having low dispersity index ($Đ = \overline{M}_w / \overline{M}_n$), and stereoregularity on the main chain. In this respect, graft or block copolymerization of thiophene onto various polymers synthesized via reversible-deactivation radical polymerization (RDRP) methods have been proposed as the first choice. As illustrated in Scheme 3, in this study the thiophene-functionalized polystyrene

was used as the macromonomer for the thiophene monomer grafts via the oxidation polymerization method.

3.1. Synthesis of thiophene-functionalized polystyrene macromonomer (ThPStM)

Macromonomers are usually referred to as reactive oligomers or polymers in which a polymerizable functional group is incorporated into the chain end(s). Macromonomers can be synthesized using various methods, including anionic, cationic and radical polymerization, as well as the chemical modification of polymer ends [39, 49]. The development of new polymeric materials usually requires the use of highly selective and efficient functionalization reactions. In this respect, Grignard reaction has been proposed as one of the most powerful tool for functionalization of polymeric materials [39, 50]. It is well established that, in comparison to corresponding carbonyl compounds, the nitrile groups are substrates not very reactive with ethereal Grignard solutions; they do not readily form the desired ketones, and the reactions often give low yields. To increase their reactivity, several researchers have used toluene or benzene as the reaction solvents, and higher temperatures could be achieved. The increase in the obtained yields was attributed to the higher temperature and not to the higher reactivity of the Grignard reagents in these solvents [51, 52].

The FTIR spectra of the PSt-*co*-PAN, and thiophene-functionalized polystyrene macromonomer (ThPStM) are shown in Figure 1. The FTIR spectrum of the PSt-*co*-PAN copolymer shows the characteristic absorption bands due to the stretching vibration of C–H (3100–2800 cm^{-1}), weak aromatic overtone and combination bands in the 1950–1650 cm^{-1} region, C=C stretching vibrations (1596 and 1478 cm^{-1}), CH_2 bending vibrations (1437 cm^{-1}), and γ(C–H) in the aromatic ring (825 and 749 cm^{-1}). Moreover, the band at

2248 cm^{-1} is attributed to the nitrile group in the FTIR spectrum of the PSt-*co*-PAN copolymer. The FTIR spectrum of the thiophene-functionalized polystyrene macromonomer (ThPStM) show similar bands with minor differences. The most distinctive features of ThPStM in comparison with PSt-*co*-PAN, in the FTIR spectra are the appearance of new bands at 1704 and 837 cm^{-1} corresponding to carbonyl and C-S groups, respectively. Moreover, the peak at 2248 cm^{-1} indicates that some of the nitrile group's does not reacted with the Grignard reagent (2-thienylmagnesium bromide).

(Figure 1)

Additional evidence for the synthesis of the thiophene-functionalized polystyrene macromonomer (ThPStM) was also obtained from ^1H nuclear magnetic resonance (NMR) spectroscopy (Figure 2). The copolymer compositions were calculated from the ^1H NMR spectra data. In the past few decades ^1H NMR spectroscopic analysis has been established as a powerful tool for the determination of copolymer compositions because of its simplicity, rapidity, and sensitivity [3, 39, 49]. The molar compositions of styrene and acrylonitrile in the synthesized copolymer were calculated from the ratio integrated intensities of the peaks around 3.75 ppm, corresponding to one methine proton (–CH-CN) of acrylonitrile units to the total area between 0.85 and 2.55 ppm, which were attributed to five aliphatic protons in acrylonitrile and styrene units. The acrylonitrile and styrene contents in the synthesized copolymer were calculated from equations (1) and (2), where x and y are the mole fractions of acrylonitrile and styrene, respectively.

1. $$\frac{\text{Area at } 3.75}{\text{Area at } 0.85 - 2.55} = \frac{x}{2x + 3y}$$

2. x+y =1

In ^{1}H NMR spectrum of the PSt-*co*-PAN, solving the simultaneous equations with the integrated areas, it can be seen that the molar compositions of styrene and acrylonitrile in the synthesized copolymer are 96.1% and 3.9%, respectively.

The ^{1}H NMR spectrum of the thiophene-functionalized polystyrene macromonomer (ThPStM) show similar peaks with minor differences. The most distinctive features in the ^{1}H NMR spectra of ThPStM and PSt-*co*-PAN are the appearance of two new peaks at 2.85 and 2.80 ppm, corresponding to –CH–C=O (i), and $–CH_2$ (h) protons, respectively. The peak at 3.75 ppm (d) indicates that some of the nitrile group's does not reacted with 2-thienylmagnesium bromide. Furthermore, before introducing thiophene groups to the PSt-*co*-PAN, the molar compositions of acrylonitrile in the copolymer was 3.9%; after introducing thiophene groups a decrease (to 3.2%) in the molar compositions of acrylonitrile in the macromonomer, according to the calculation using equations (1) and (2), can be attributed to the fact that the thiophene groups were introduced into the PSt-*co*-PAN, and that the ThPStM was successfully synthesized. Therefore, the extent of thiophene groups in the macromonomer (ThPStM) is 3.9% – 3.2% = 0.7%. Additionally, we can report that 17.9% of the nitrile groups in the PSt-*co*-PAN were converted to thiophene groups. These results show that, the yield of ketone in the reaction between nitrile groups of acrylonitrile units and 2-thienylmagnesium bromide (Grignard reagent) was 17.9%. We propose that the use of high boiling point solvents such as toluene in the both steps (preparation of Grignard reagent and Grignard reaction) of this procedure may be the best and first choice for the increasing of the yield.

(Figure 2)

3.2. Synthesis of PSt-*g*-PTh

Two kinds of cation radicals initiate thiophene polymerization after addition of $FeCl_3$. One is oxidized thiophene groups coupled to the polystyrene backbone; the other is oxidized thiophene cation radicals. As reaction time increasing, more thiophene monomers join in the polymerization. Some are entrapped into the polymer chains initiated by oxidized thiophene groups coupled to the polystyrene backbone; others incorporate the polymer chains initiated by oxidized thiophene cation radicals. This polymer chains could not be linked chemically to the polystyrene backbone. To remove the ungrafted polystyrene and pure PTh chains, the crude product was purified as described in the experimental section.

Atom transfer radical polymerization (ATRP) is well established as a reversible-deactivation radical polymerization (RDRP) methodology that enables the design of well-defined, functional, and complex macromolecular architectures with a narrow molecular weight distribution under mild conditions. Table I represents the molecular weights analysis data of PSt-*co*-PAN, and PSt-*g*-PTh copolymers by GPC. The molecular weight distributions of PSt-*co*-PAN, and PSt-*g*-PTh copolymers were obtained 1.24 and 1.44, respectively. As shown in Figure 3 the GPC chromatograms of PSt-*co*-PAN (a), and PSt-*g*-PTh (b) copolymers verify that, polythiophene was chemically grafted onto polystyrene backbone because the chromatogram of the PSt-*g*-PTh is shifted to higher molecular weight compared with the chromatogram of PSt-*co*-PAN copolymer. Moreover, the single peak of the chromatogram of the PSt-*g*-PTh graft copolymer indicates that the product cannot be a blend of PSt-*co*-PAN, and PTh; if so, the chromatogram should

appear as two peaks, one for PSt-*co*-PAN, and the other for PTh. Thus the PSt-*g*-PTh graft copolymer was successfully synthesized according to the GPC chromatograms.

(TableI)

(Figure 3)

The FTIR spectra of the PSt-*g*-PTh graft copolymer and pure PTh are shown in Figure 4. The FTIR spectrum of pure PTh shows the characteristic absorption bands due to the stretching vibration of C=C (1568 and 1452 cm^{-1}), γ(C–H) in the aromatic ring (1004 and 768 cm^{-1}), and the C–S bending band at 741 cm^{-1}. The FTIR spectrum of the PSt-*g*-PTh shows all the characteristic peaks of polystyrene and also the peaks attributable to PTh.

(Figure 4)

Additional evidence for the synthesis of the PSt-*g*-PTh was also obtained from ^{1}H NMR data (Figure 5). The extent of polythiophene in the graft copolymer was calculated from the ^{1}H NMR data to be 21.05% (See Supporting Information).

(Figure 5)

3.3. Thermal property study

The thermal behaviors of the PSt-*co*-PAN, PTh, and PSt-*g*-PTh were examined by means of differential scanning calorimetry (DSC), and thermogravimetric analysis (TGA). The DSC traces of the PSt-*co*-PAN, PTh, and PSt-*g*-PTh are shown in Figure 6. The PSt-*co*-PAN copolymer is a non-crystalline polymer and therefore does not exhibit any crystallization or melting transitions. The DSC curve of PSt-*co*-PAN exhibits a weak endothermic peak at approximately 85 °C, corresponding to the glass transition temperature (T_g) of the copolymer. In the DSC curve of PTh it can be seen that the main degradation of the PTh occur around 220-290 °C. In contrast to the DSC patterns of

semicrystalline polymer systems, the DSC thermogram for PTh did not show any peaks indicative of phase transitions from room temperature to 430 °C. The DSC curve of the PSt-*g*-PTh graft copolymer did not show any peaks indicative of phase transitions. In addition, the T_g is too weak to measure, or it is suppressed due to the confinements of polystyrene chains by polythiophene segments.

(Figure 6)

The thermal behaviors of the PSt-*co*-PAN, PTh, and PSt-*g*-PTh upon heating in nitrogen atmosphere were investigated by TGA. As shown in Figure 7 the TGA curve of the PSt-*co*-PAN copolymer exhibits a two-step weight loss process; the first step corresponds to the decomposition of the PAN chains (250–310 °C), whereas the second step is associated with the PSt chains scission (310–420 °C), after which the loss rate slows down. In the case of pure PTh, decomposition occur in one step at around 230–400, after which the loss rate slows down. However, the thermal decomposition of the PSt-*g*-PTh graft copolymer in nitrogen atmosphere occur in a two-step; the first step corresponds to the decomposition of the PTh chains (240–320 °C), whereas the second step is associated with the PSt chains scission (330–420 °C), after which the loss rate slows down. In addition, it is important to note that PAN and PTh have overlapping (240–320 °C), degradation process in the TGA curve of the graft copolymer. The residue at 800 °C for the synthesized samples, obtained from the TGA curves are summarized in Table II.

(Figure 7)

(Table II)

3.4. Solubility test

The solubility of the PSt-*g*-PTh graft copolymer and pure PTh in common organic solvents are summarized in Table III. Polystyrene has excellent solubility in non-polar solvents. The solubility of PSt-*g*-PTh in common organic solvents improved compared to pure PTh, because thiophene has grown onto polystyrene backbone.

(Table III)

3.5. Electrical conductivity and electroactivity measurements

Unlike to other type of polymers, π-conjugated polymers exhibit conducting and/or semiconducting behaviors and thus serve as potential candidates for both optical and electronic applications. The electrical resistivity (R) of the synthesized samples, was measured at room temperature and then converted to volume specific resistivity (ρ) using the equation $R = \rho L/A$. In this equation, A is the test sample cross-section area, and L the sample thickness. Finally, the electrical conductivity (σ) is the reciprocal of ρ ($\sigma = 1/\rho$). The electrical conductivity values (σ) of the pure PTh and PSt-*g*-PTh were obtained 0.24 and 0.11 S cm^{-1}, respectively.

The effect of the potential scanning rate (V) on the peak current for the pure PTh and PSt-*g*-PTh modified electrodes was studied in the acetonitrile–tetraethylammonium tetrafluoroborate (TBAFB), solvent-electrolyte couple (0.1 mol L^{-1}), by applying a sequential linear potential scan rate of 25–175 mVs^{-1} between 0.00 and +1.50 V *versus* the Ag/AgCl electrode (Figure 8). The polymer films were prepared on the platinum electrode by casting. As shown in Figure 8b, when cyclic voltammograms (CVs) of the pure PTh film are recorded between 0.0 and +1.5 V *versus* Ag/AgCl at a scan rate of 25–175 mVs^{-1}, the oxidation and reduction peak currents are observed at approximately 0.91

and 1.18 V *versus* Ag/AgCl, respectively. Moreover, the anodic peaks shifts in the direction of positive potential with increasing scan rate, which indicates the electrochemical oxidation/reduction (doping/dedoping) of the casted PTh film was chemically reversible. The CVs of the PSt-*co*-PAN copolymer does not exhibit any detectable redox peak. Figure 8a shows that the PSt-*co*-PAN sample is a non-electroactive polymer.

As shown in Figure 8c, CVs of PSt-*g*-PTh exhibit some qualitative similarities to those of pure PTh. The CVs of PSt-*g*-PTh exhibited that the grafted PTh onto PSt backbone still retained good redox activity in the resulting graft copolymer, and the resulting graft copolymer was highly stable. Furthermore, similar to cyclic voltammograms of pure PTh for PSt-*g*-PTh the anodic peak current is linearly increased with increasing of scan rate.

To evaluate the electroactivity further the relationship between the peak current sizes *versus* scan rate was determined. Figure 8d shows linear relationships between the current and scan rate between 25–175 mVs^{-1} for PSt-*g*-PTh and PTh. This linear relationship is typical of redox-active polymers attached to the electrodes and also exemplifies the stability of PSt-*g*-PTh and PTh films toward doping/dedoping.

For additional evidence, the cyclic voltammograms (15 cycles) of pure PTh and PSt-*g*-PTh are recorded between 0.0 and +1.4 V *versus* Ag/AgCl at a scan rate of 300 mVs^{-1}. As shown in Figure 9 the oxidation and reduction peak currents for pure PTh film are observed at approximately 0.86 and 1.3 V *versus* Ag/AgCl, respectively. When cyclic voltammograms (CVs) of the PSt-*g*-PTh are recorded at a scan rate of 300 mVs^{-1}, can be seen that the oxidation and reduction peak currents are observed at approximately 0.83 and 1.25 V *versus* Ag/AgCl, respectively. The relatively similar cyclic voltammograms

of pure PTh and PSt-*g*-PTh verify the formation of graft copolymer (PSt-*g*-PTh), in accordance with the results obtained by other means of characterizations.

On the bases of the evidence from electrical conductivity and electroactivity measurements the conclusion could be drawn that the PSt-*g*-PTh exhibits lowers electrical conductivity and electroactivity than those of the pure PTh due to the decreased conjugation length distribution. However, the lowers electrical conductivity and electroactivity levels in the modified PTh can be improved at the price of solubility and processability.

(Figure 8)

(Figure 9)

3.6. UV–visible spectroscopy

The optical properties of the samples were studied using ultraviolet–visible (UV–vis) spectroscopy. The samples for UV–vis spectroscopy were prepared by dissolving the same amount of the obtained polymers in dimethylsulfoxide (DMSO) followed by ultrasonic treatment for 10 minutes. Figure 10 shows the UV–visible spectra of the pure PTh and PSt-*g*-PTh graft copolymer dissolved in dimethylsulfoxide solution. The UV–visible spectrum of PTh was characterized by two electronic transitions at about 341 and 619 nm, while the UV–visible spectrum of the PSt-*g*-PTh was characterized by only one electronic transition at about 527 nm, being lower than pure PTh. This shift to shorter wavelength (blue shift) is ascribed to the significantly lower concentration of conjugated units in the case of PSt-*g*-PTh in comparison with pure PTh [39].

(Figure 10)

4. Conclusion

This work has shown an efficient and novel approach for the synthesis of conductive polythiophene copolymer via a combination of atom transfer radical polymerization (ATRP), and Grignard reaction. The growth of thiophene onto functionalized polystyrene enhanced its solubility and processability compared with pure polythiophene. Investigation of thermal behaviors of the PSt-*g*-PTh graft copolymer showed the increased flexibility compared with pure PTh due to the grafting process. The cyclic voltammograms (CVs) of the PSt-*g*-PTh exhibited some qualitative similarities with those of pure PTh. The CVs of PSt-*g*-PTh indicated that the grafted polythiophene onto polystyrene backbone still remained a good redox activity in the resulting graft copolymer, and the synthesized graft copolymer was high stable. The PSt-*g*-PTh exhibited lowers electrical conductivity and electroactivity than those of the pure PTh due to the decreased conjugation length distribution. However, the lowers electrical conductivity and electroactivity levels in the PSt-*g*-PTh can be improved at the price of solubility and processability. The synthesized PSt-*g*-PTh showed the polaronic band, at lower wavelength (higher energy) than pure PTh in the UV-vis spectra due to lower concentration of conjugated units in the case of PSt-*g*-PTh.

Acknowledgments

We express our gratitude to the Research Center for Pharmaceutical Nanotechnology, Tabriz University of Medical Sciences and Payame Noor University for supporting this project.

Supporting Information

Information is available regarding the calculation of copolymer (PSt-*g*-PTh) compositions from the ^{1}H NMR data.

References

[1] C. Gao, B. Qu, D. Chen, Z. Cong, J. Liu, J. Chen, Z. An, Z. Chen, L. Xiao, W. Wei and Q. Gong, *Reac. Funct. Polym.,* 2012, **72**, 122–126.

[2] M. Sangermano, F. Sordo, A. Chiolerio and Y. Yagci, *Polymer,* 2013, **54**, 2077-2080.

[3] M. Hatamzadeh, A. Mahyar and M. Jaymand. *J. Braz. Chem. Soc.,* 2012, **23**, 1008–1017.

[4] M. Jaymand, *Design. Monomer. Polym.,* 2011, **14**, 433–444.

[5] M. Jaymand, *Prog. Polym. Sci.,* 2013, **38**, 1287–1306.

[6] M. Jaymand, *Polymer(Korea),* 2010, **34**, 553-559.

[7] S. Jayaraman, P. S. Kumar, D. Mangalaraj, D. Rajarathnam, S. Ramakrishna and M. P. Srinivasan, *RSC Adv.,* 2014, **4**, 11288-11294.

[8] M. Shao, Y. He, K. Hong, C. M. Rouleau, D. B. Geohegan and K. Xiao, *Polym. Chem.,* 2013, **4**, 5270-5274.

[9] C. Lai, W. Guo, X. Tang, G. Zhang, Q. Pan and M. Pei, *Synthetic. Met.,* 2011, **161**, 1886–1891.

[10] H. W. Ryu, Y. S. Kim, J. H. Kim and I. W. Cheong, *Polymer,* 2014, **55**, 806–812.

[11] B. Yaman, I. Terkesli, K. M. Turksoy, A. Sanyal and S. Mutlu. *Org. Electron.,* 2014, **15**, 646–653.

[12] S. Samanta, D. P. Chatterjee, R. K. Layek and A. K. Nandi, *J. Mater. Chem.,* 2012, **22**, 10542–10551.

[13] L. Cardenas, R. Gutzler, J. Lipton-Duffin, C. Fu, J. L. Brusso, L. E. Dinca, M. Vondráček, Y. Fagot-Revurat, D. Malterre, F. Rosei and D. F. Perepichka, *Chem. Sci.,* 2013, **4**, 3263-3268.

[14] H. N. Kim, Z. Guo, W. Zhu, J. Yoon and H. Tian, *Chem. Soc. Rev.,* 2011, **40**, 79–93.

[15] X. Li, Y. Wang, X. Yang, J. Chen, H. Fu and T. Cheng, *Trend. Anal. Chem.,* 2012, **39**, 163-179.

[16] H. J. Wang, Y. P. Chen, Y. C. Chen, C. P. Chen, R. H. Lee, L. H. Chan and R. J. Jeng, *Polymer,* 2012, **53**, 4091-4103.

[17] T. Higashihara and M. Ueda, *Macromol. Res.,* 2013, **21**, 257-271.

[18] T. Bilkay, K. Schulze, T. Egorov-Brening, A. Bohn and S. Janietz, *Macromol. Chem. Phys.,* 2012, **213**, 1970−1978.

[19] Y. Hosokawa, M. Misaki, S. Yamamoto, M. Torii, K. Ishida and Y. Ueda, *Appl. Phys. Lett.,* 2012, **100**, 203305.

[20] S. K. Ahn, T. Ban, P. Sakthivel, S. H. Jin, Y. S. Gal and J. H. Lee, *Macromol. Res.,* 2012, **20**, 459-464.

[21] J. Shen, H. Masaoka, K. Tsuchiya and K. Ogino, *Polym. J.,* 2008, **40**, 421–427.

[22] N. K. Guimard, N. Gomez and C. E. Schmidt, *Prog. Polym. Sci.,* 2007, **32**, 876–921.

[23] D. Mawad, E. Stewart, D. L. Officer, T. Romeo, P. Wagner, K. Wagner and G. G. Wallace, *Adv. Funct. Mater.,* 2012, **22**, 2692–2699.

[24] J. M. Pringle, M. Forsyth, D. R. Mac-Farlane, K. Wagner, S. B. Hall and D. L. Officer, *Polymer,* 2005, **46,** 2047–2058.

[25] M. D. Levi and D. Aurbach, *J. Power. Sources.,* 2008, **180**, 902–908.

[26] S. Tamba, Y. Okubo, A. Sugie and A. Mori, *Polym. J.,* 2012, **44**, 1209–1213.

[27] S. Kowalski, S. Allard, K. Zilberberg, T. Riedl and U. Scherf, *Prog. Polym. Sci.,* 2013, **38**, 1805–1814.

[28] S. S. Jeon, S. J. Yang, K. J. Lee and S. S. Im, *Polymer,* 2010, **51**, 4069-4076.

[29] C. Y. Kuo, Y. C. Huang, C. Y. Hsiow, Y. W. Yang, C. I. Huang, S. P. Rwei, H. L. Wang and L. Wang, *Macromolecules,* 2013, **46**, 5985-5997.

[30] L. Angiolini, A. Brazzi, E. Salatelli, K.V. Bergh and G. Koeckelberghs, *Macromol. Chem. Phys.,* 2013, **214**, 934−942.

[31] G. Lu, L. Li and X. Yang, *Macromolecules,* 2008, **41**, 2062-2070.

[32] E. Grana, D. Katsigiannopoulos, A. E. Karantzalis, M. Baikousi and A. Avgeropoulos, *Euro. Polym. J.,* 2013, **49**, 1089–1097.

[33] J. Malmstro□m, M. K. Nieuwoudt, L. T. Strover, A. Hackett, O. Laita, M. A. Brimble, D. E. Williams and J. Travas-Sejdic, *Macromolecules,* 2013, **46**, 4955−4965.

[34] C. Muller, C. P. Radano, P. Smith and N. Stingelin-Stutzmann, *Polymer,* 2008, **49**, 3973–3978.

[35] B. W. Boudouris, C. D. Frisbie and M. A. Hillmyer, *Macromolecules,* 2010, **43**, 3566–3569.

[36] Y. Gune, L. Toppare, Y. Hepuzer and Y. Yagci, *Euro. Polym. J.,* 2004, **40**, 1799–1806.

[37] I. Erol and Ö. Arslan, *J. Biomater. Sci: Polym. Ed.,* 2013, **24**, 1198–1218.

[38] J. Shen, K. Tsuchiya and K. Ogino, *J. Polym. Sci: Polym. Chem.,* 2008, **43**, 1003–1013.

[39] M. Hatamzadeh, M. Jaymand and B. Massoumi, *Polym. Int.,* 2014, **63**, 402-412.

[40] J. S. Wang and K. Matyjaszewski, *Macromolecules,* 1995, **28**, 7901–7910.

[41] T. Von-Werne and TE. Patten, *J. Am. Chem. Soc.,* 1999, **121**, 7409–7410.

[42] M. Jaymand, *J. Polym. Res.,* 2011, **18**, 1617–1624.

[43] M. Jaymand, *Macromol. Res.,* 2011, **19**, 998-1005.

[44] A. D. Jenkins, R. G. Jones, and G. Moad, *Pure Appl. Chem.,* 2010, **82**, 483–491.

[45] K. T. Kim and W. H. Jo, *Compos. Sci. Technol.,* 2009, **69**, 2205–2211.

[46] Y. Tao, B. Mc-Culloch, S. Kim and R. A. Segalman, *Soft. Matter.,* 2009, **5**, 4219–4230.

[47] L. Strover, C. Roux, J. Malmström, Y. Pei, D. E. Williams and J. Travas-Sejdic, *Synthetic. Met.,* 2012, **162**, 381–390.

[48] S. Das, S. Samanta, D. P. Chatterjee and A. K. Nandi, *J. Polym. Sci: Polym. Chem.,* 2013, **51**, 1417–1427.

[49] M. Jaymand, *Polym. J.,* 2011, **43**, 901–908.

[50] F. Monnaie, W. Brullot, T. Verbiest, J. D. Winter, P. Gerbaux, A. Smeets and G. Koeckelberghs, *Macromolecules,* 2013, **46**, 8500-8508.

[51] J. Pawlas and M. Begtrup, *Org. Lett.,* 2002, **4**, 2687–2690.

[52] M. S. Kharasch and O. Reinmuth, Grignard reactions of Nonmetallic Substances. *Prentice-Hall, Inc., New York.,* 1954, 769-772.

Captions:

Scheme 1. Synthesis of poly(styrene-*co*-acrylonitrile) via ATRP technique.

Scheme 2. Synthesis of thiophene-functionalized polystyrene macromonomer (ThPStM).

Scheme 3. Graft copolymerization of thiophene onto thiophene-functionalized polystyrene macromonomer (ThPStM).

Scheme 4. Synthesis of pure polythiophene.

Figure 1. Fourier transform infrared spectra of the PSt-*co*-PAN, and thiophene-functionalized polystyrene macromonomer (ThPStM).

Figure 2. ^{1}H nuclear magnetic resonance (NMR) spectra of PSt-*co*-PAN, and thiophene-functionalized polystyrene macromonomer (ThPStM).

Table I. Molecular weights' analysis data of PSt-*co*-PAN, and PSt-*g*-PTh copolymers by GPC.

Figure 3. GPC chromatograms of PSt-*co*-PAN (a), and PSt-*g*-PTh (b) copolymers.

Figure 4. Fourier transform infrared spectra of the PSt-*g*-PTh graft copolymer and pure PTh.

Figure 5. ^{1}H nuclear magnetic resonance (NMR) spectrum of PSt-*g*-PTh.

Figure 6. Differential scanning calorimeter traces of the PSt-*co*-PAN, PTh, and PSt-*g*-PTh.

Figure 7. Thermogravimetric analysis of the PSt-*co*-PAN, PTh, and PSt-*g*-PTh.

Table II. The residue at 800 °C for PSt-*co*-PAN, PTh, and PSt-*g*-PTh.

Table III. Solubility of pure PTh and PSt-*g*-PTh in common organic solvents.

Figure 8. Cyclic voltammograms (CVs) of (a) pure PSt-*co*-PAN, (b) neat PTh and (c) PSt-*g*-PTh, and (d) the linear relationship between current and scan rate in PTh (curve (1)) and PSt-*g*-PTh (curve (2)).

Figure 9. Cyclic voltammograms of pure PTh and PSt-*g*-PTh at a scan rate of 300 mVs^{-1}.

Figure 10. Absorption spectra of PTh and PSt-*g*-PTh in dimethylsulfoxide (DMSO) solution.

Schemes, Figures, and Tables:

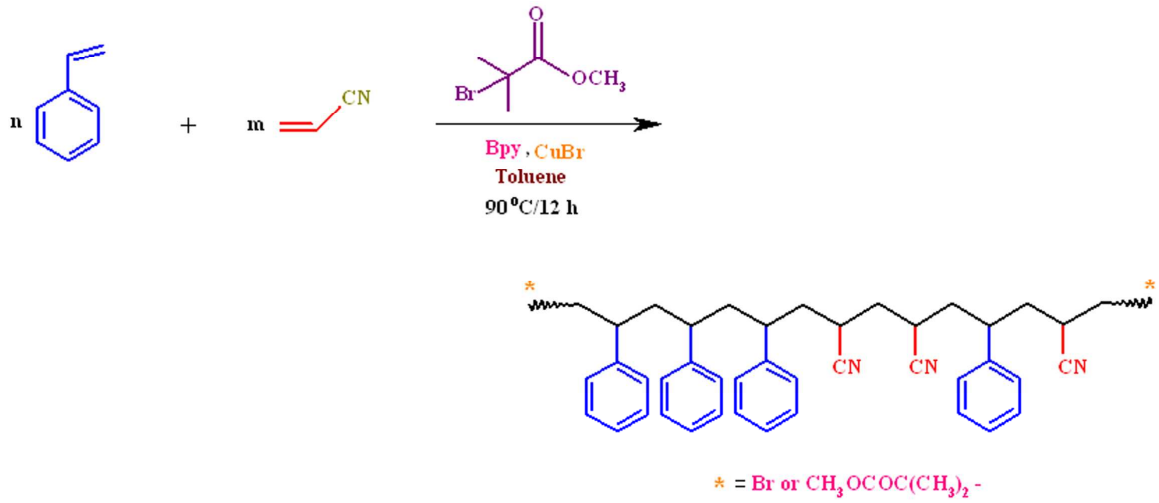

Scheme 1. Synthesis of poly(styrene-*co*-acrylonitrile) via ATRP technique.

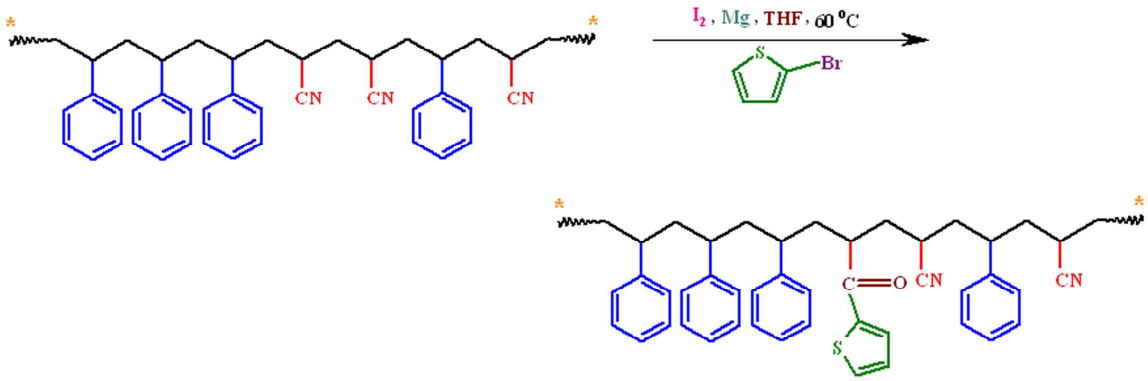

Scheme 2. Synthesis of thiophene-functionalized polystyrene macromonomer (ThPStM).

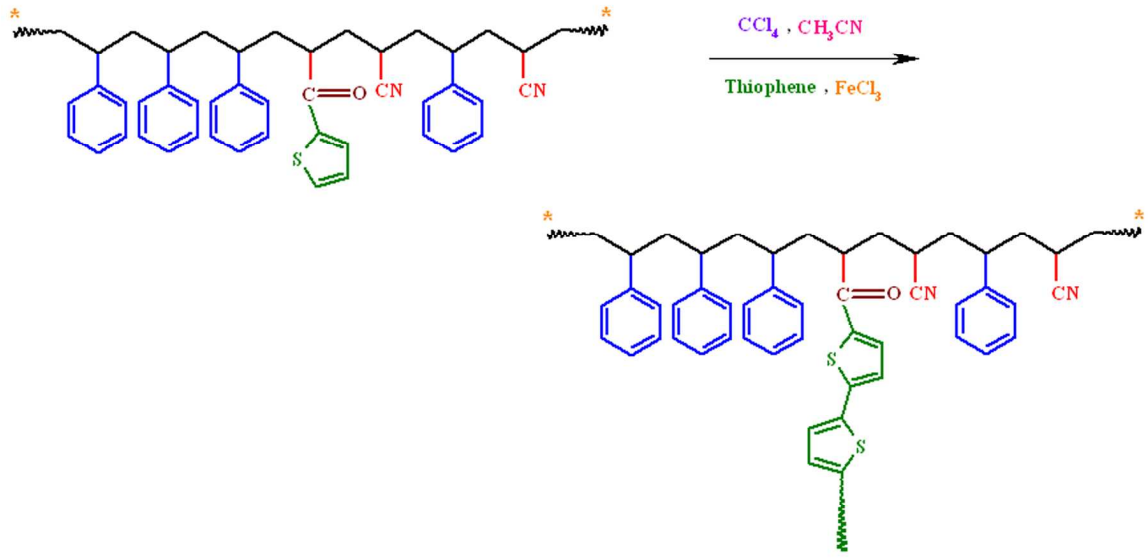

Scheme 3. Graft copolymerization of thiophene onto thiophene-functionalized polystyrene macromonomer (ThPStM).

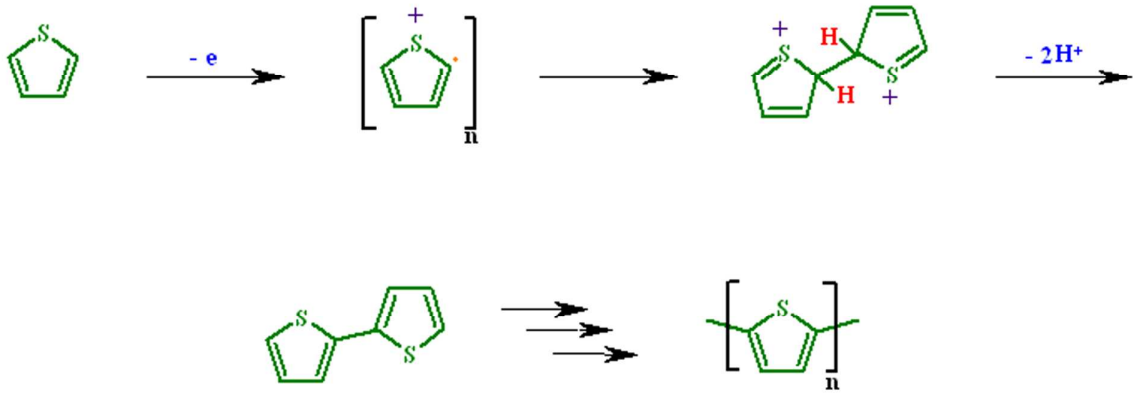

Scheme 4. Synthesis of pure polythiophene.

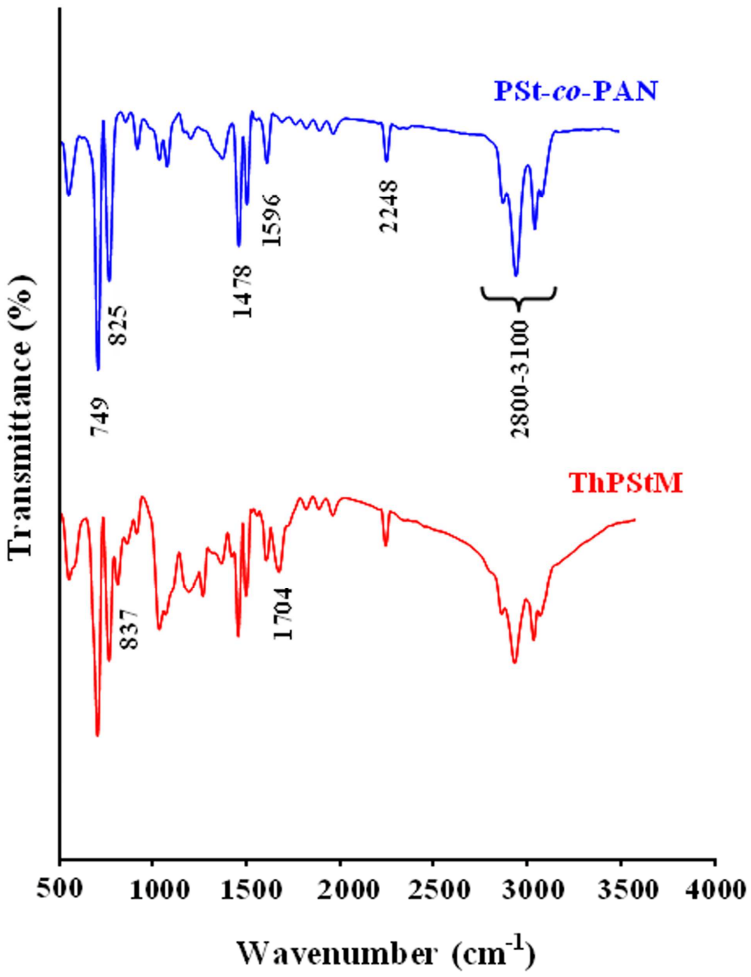

Figure 1. Fourier transform infrared spectra of the PSt-*co*-PAN, and thiophene-functionalized polystyrene macromonomer (ThPStM).

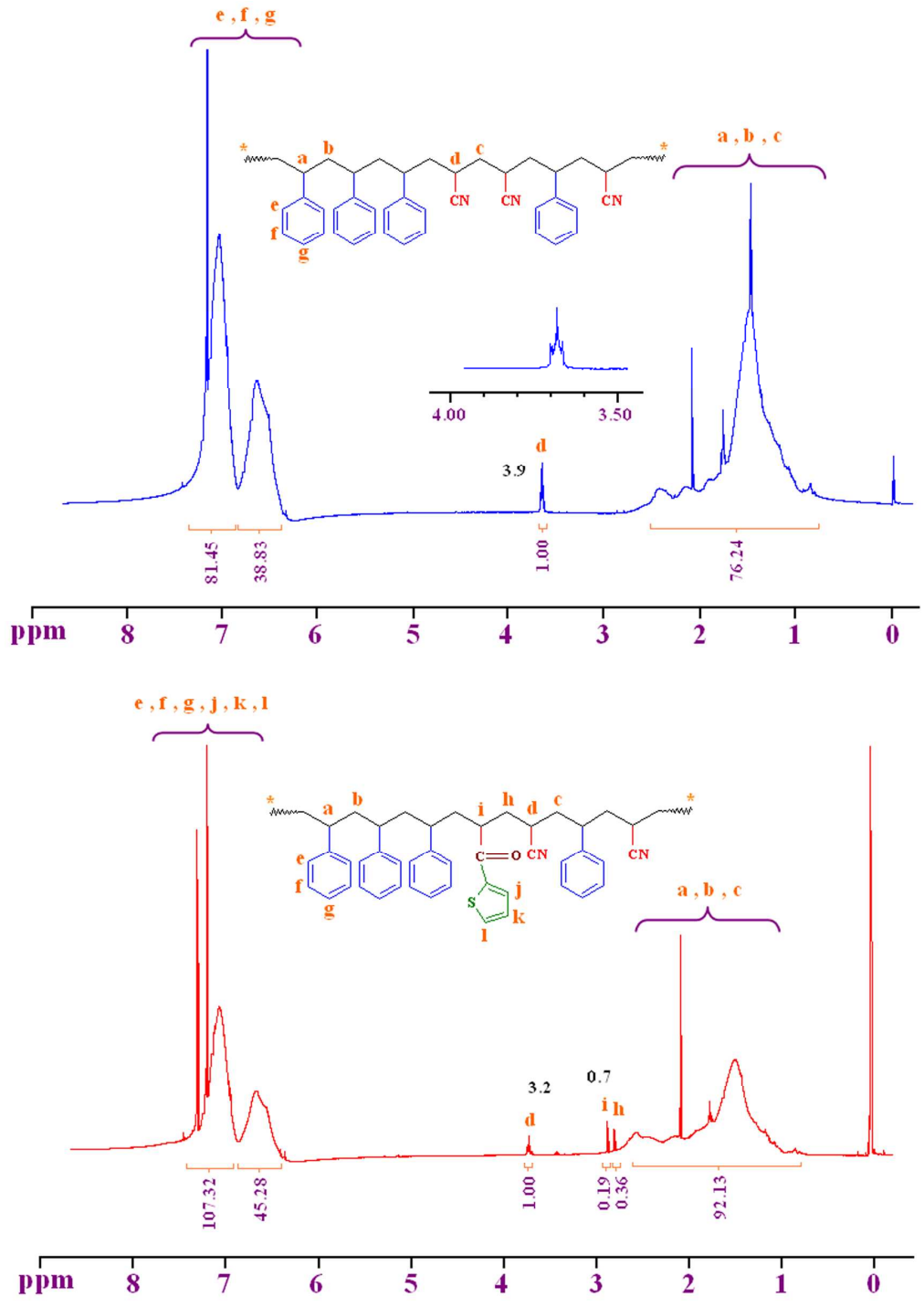

Figure 2. [1]H nuclear magnetic resonance (NMR) spectra of PSt-*co*-PAN, and thiophene-functionalized polystyrene macromonomer (ThPStM).

Table I. Molecular weights' analysis data of PSt-*co*-PAN, and PSt-*g*-PTh copolymers by GPC.

Samples	$\overline{M}n$	$\overline{M}w$	Đ = $\overline{M}_w / \overline{M}_n$	PSt-*co*-PAN [%][a]	PTh [%][a]
PSt-*co*-PAN	15846	19682	1.24	100	-
PSt-*g*-PTh	19037	27513	1.44	79.8	20.1

[a] Composition calculated from the $\overline{M}_n$ values of the starting polystyrene sample and the resulting graft copolymer.

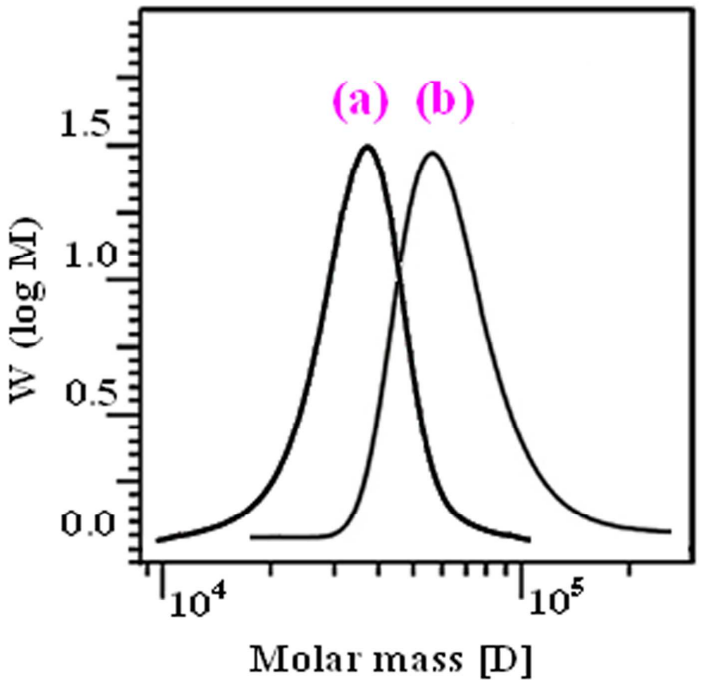

Figure 3. GPC chromatograms of PSt-*co*-PAN (a), and PSt-*g*-PTh (b) copolymers.

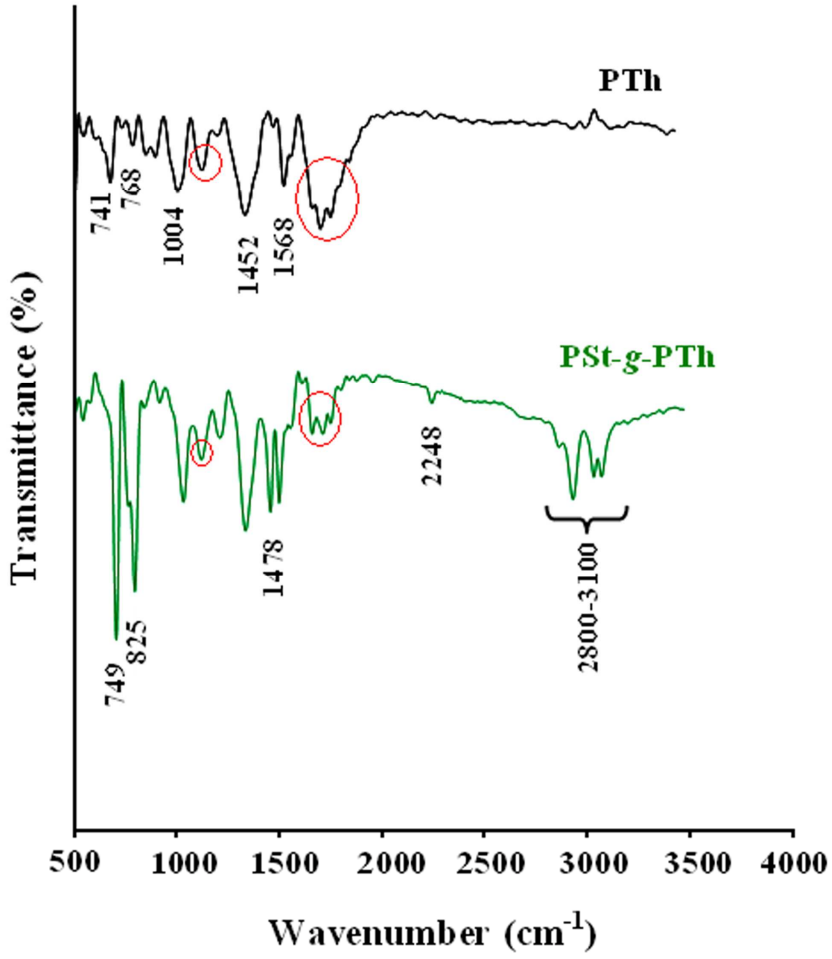

Figure 4. Fourier transform infrared spectra of the PSt-*g*-PTh graft copolymer and pure PTh.

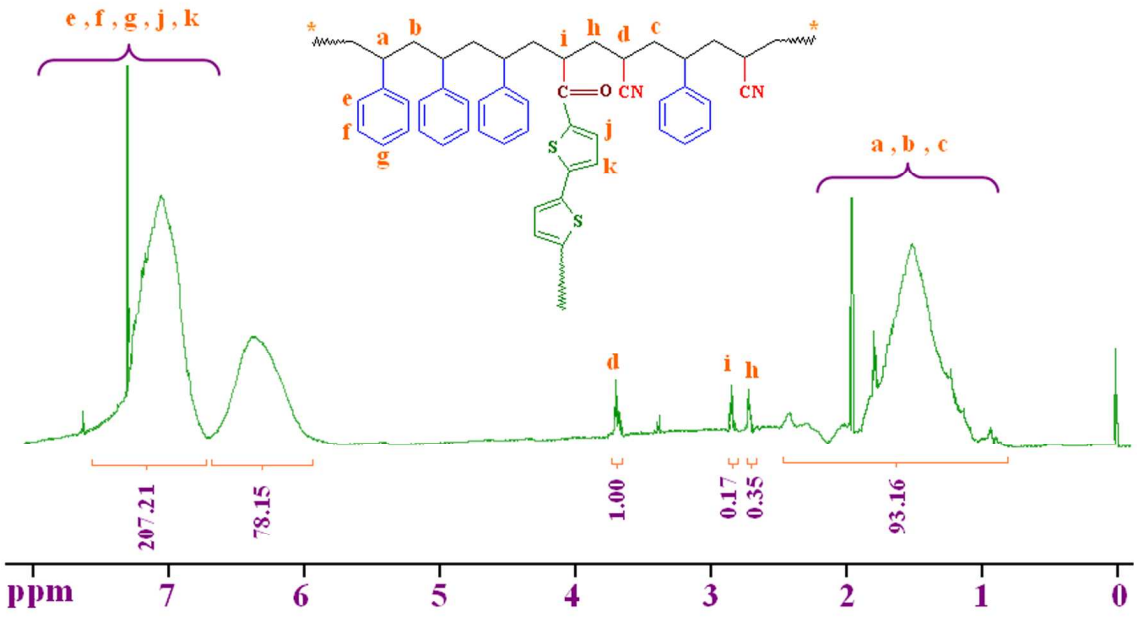

Figure 5. ^{1}H nuclear magnetic resonance (NMR) spectrum of PSt-*g*-PTh.

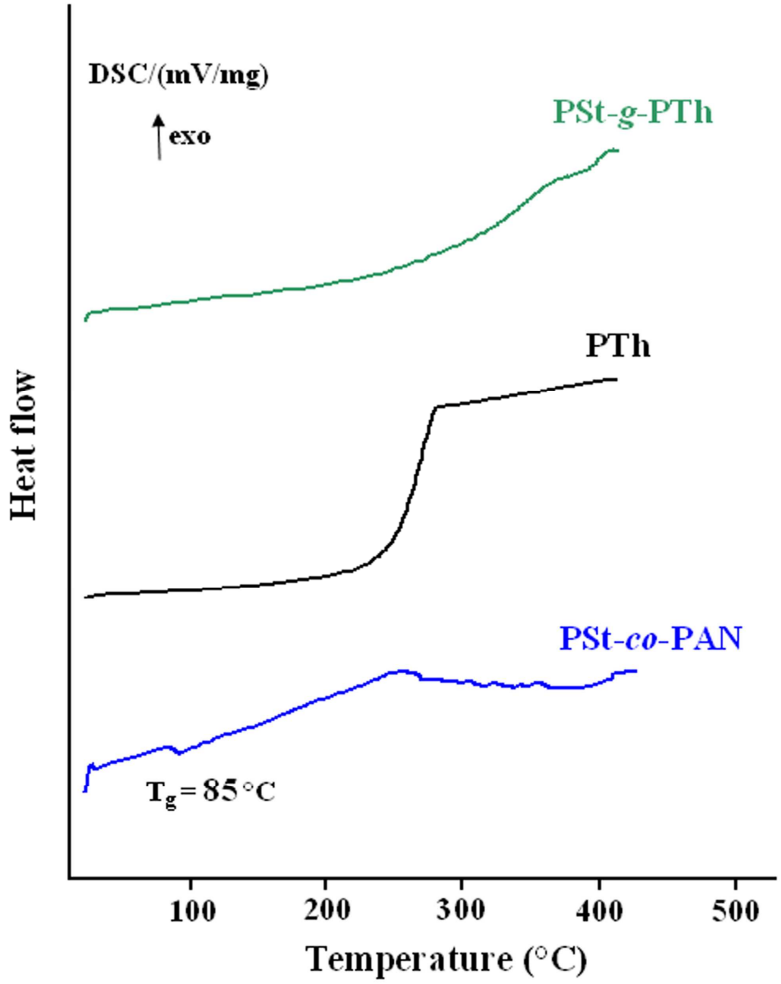

Figure 6. Differential scanning calorimeter traces of the PSt-*co*-PAN, PTh, and PSt-*g*-PTh.

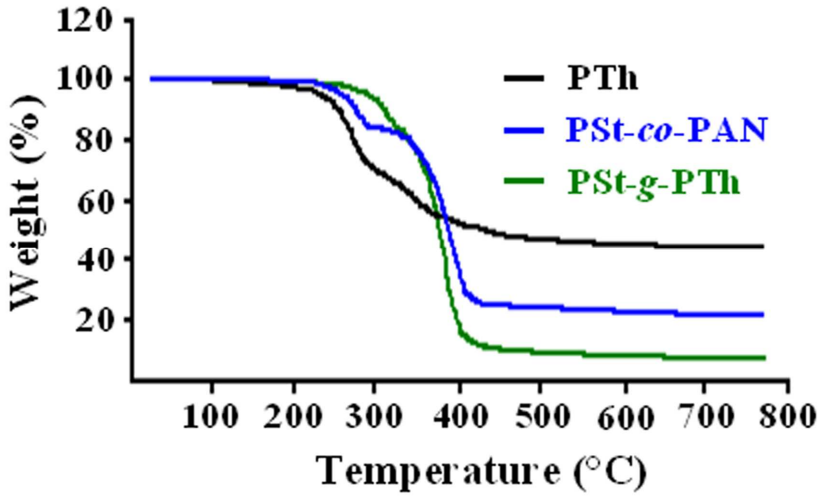

Figure 7. Thermogravimetric analysis of the PSt-*co*-PAN, PTh, and PSt-*g*-PTh.

Table II. The residue at 800 °C for PSt-*co*-PAN, PTh, and PSt-*g*-PTh.

Sample	Initial (wt%)	Residual at 800 °C (wt%)
PSt-*co*-PAN	100	7
PTh	100	42
PSt-*g*-PTh	100	21

Table III. Solubility of pure PTh and PSt-*g*-PTh in common organic solvents.

Solvent	DMSO	NMP	THF	$CHCl_3$	Xylene	DMF
PTh	+	+	-	-	-	+
PSt-*g*-PTh	+ + +	+ + +	+ + +	+ +	+ +	+ + +

+ + +: soluble; + +: sparingly soluble; +: slightly soluble; –: insoluble; the concentration used in the solubility test was 10 mg of each polymer in 1 ml of solvents (DMSO, dimethylsulfoxide; NMP, *N*-methylpyrrolidone; DMF, dimethylformamide).

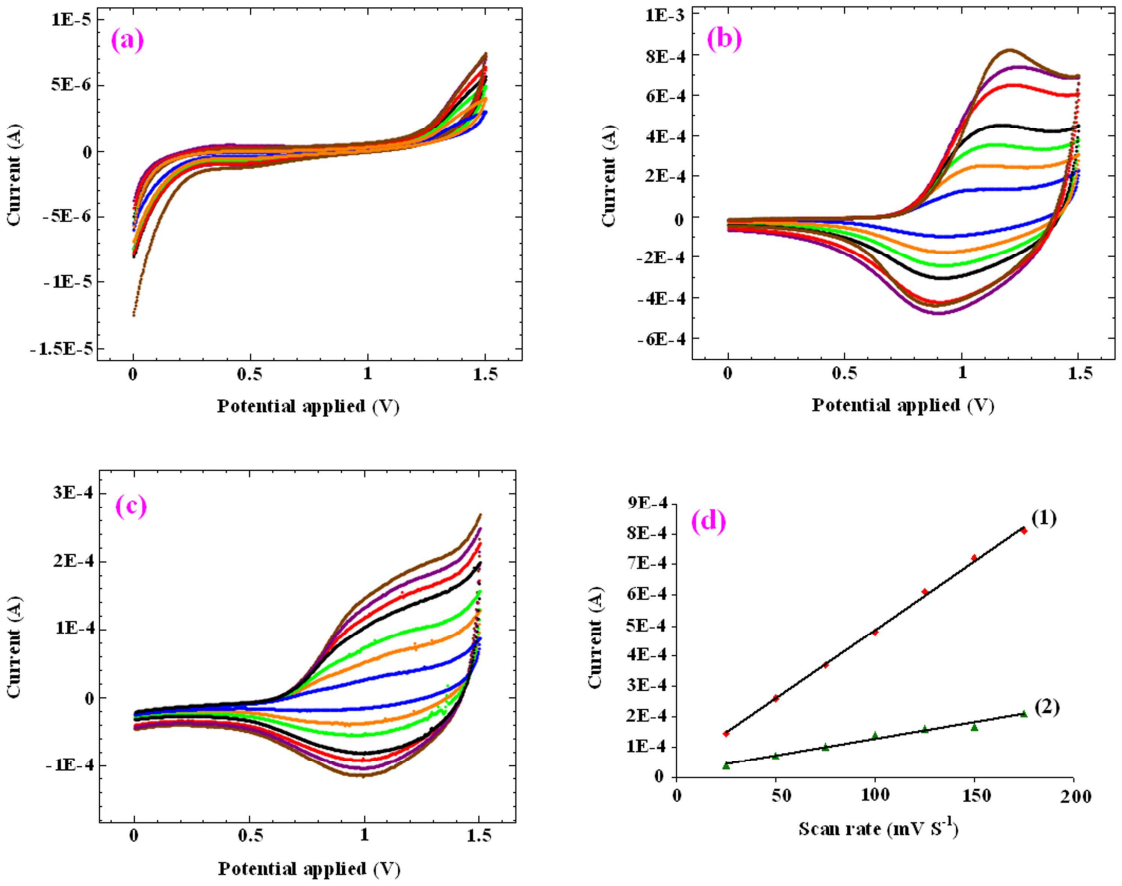

Figure 8. Cyclic voltammograms (CVs) of (a) pure PSt-*co*-PAN, (b) neat PTh and (c) PSt-*g*-PTh, and (d) the linear relationship between current and scan rate in PTh (curve (1)) and PSt-*g*-PTh (curve (2)).

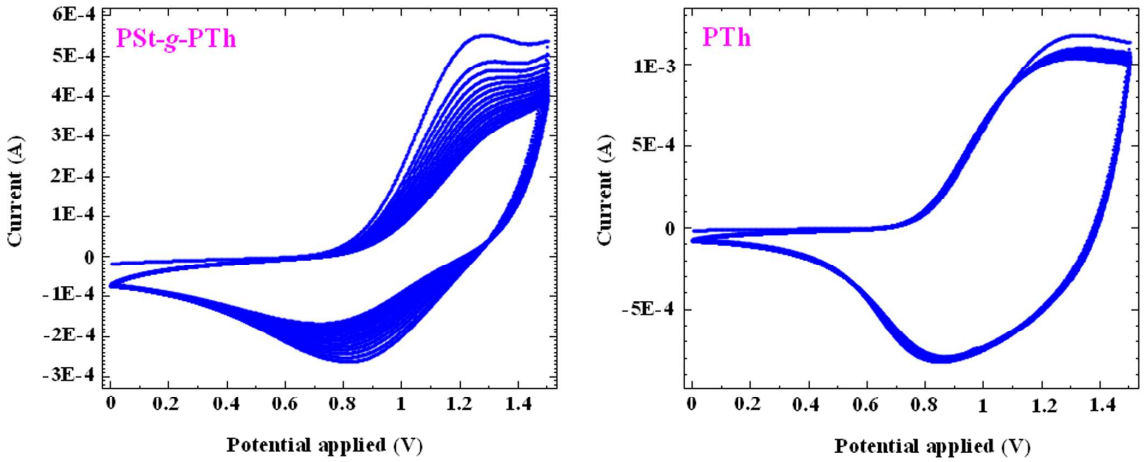

Figure 9. Cyclic voltammograms of pure PTh and PSt-*g*-PTh at a scan rate of 300 mVs^{-1}.

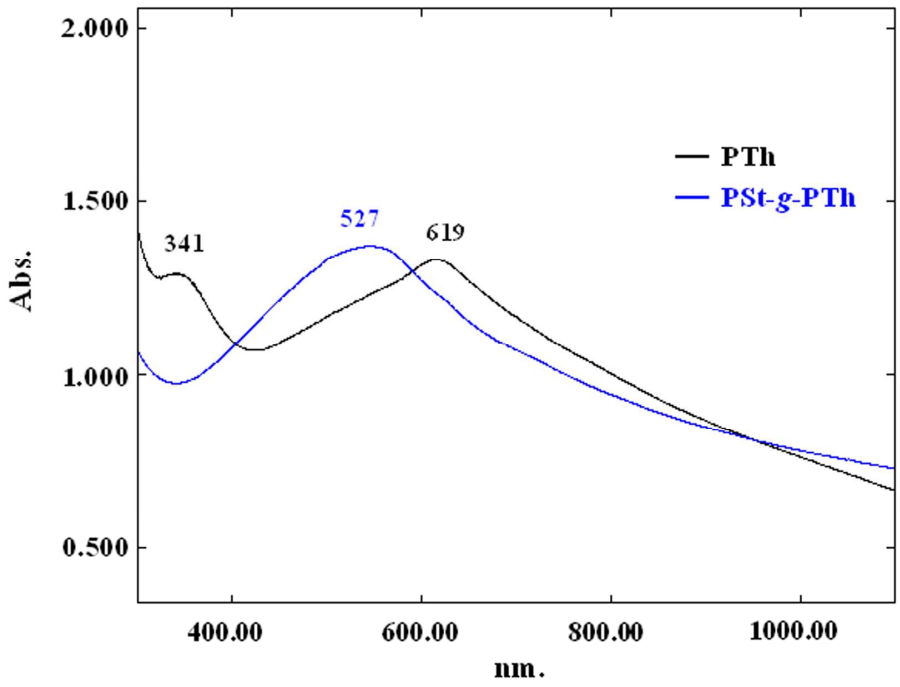

Figure 10. Absorption spectra of PTh and PSt-*g*-PTh in dimethylsulfoxide (DMSO) solution.